CHEMBIOCHEM

Supporting Information

DOI: 10.1002/cbic.200800736

Supporting Information

for

RDCs in Short Peptidic Foldamers: Combined Analyses of Backbone and Side-Chain Conformations and Evaluation of Structure Coordinates of Rigid Unnatural Amino Acids

Markus B. Schmid, Matthias Fleischmann, Valerio D´Elia, Oliver Reiser, Wolfram Gronwald, and Ruth M. Gschwind*

1. Experimental Section

Compounds **1** and **2** were synthesized following the published protocol.[1]

NMR spectra were recorded on a Bruker Avance DRX 600 spectrometer (600.13 MHz) (temperature was controlled by a BVT 3000 unit) and on a Bruker Avance III 600 (600.25 MHz) equipped with a TCI cryoprobe with z-gradient.

Sample concentrations of 40 mM to 140 mM were applied for NMR measurements of **1** at 240 K and 300 K depending on sensitivity requirements of the different spectra, while aggregation in this concentration and temperature range could be excluded by comparison of chemical shifts and by diffusion measurements with convection artefact suppression.[2] Due to the relatively small size of the investigated molecules and therefore slow NOE build-up a mixing time of 350 ms had to be used in the 2D ^{1}H,^{1}H-NOESY spectra. ^{1}H,^{13}C-P.E.HSQC[3] spectra for the determination of RDCs were measured in $CDCl_3$ and in a strained $CDCl_3$/PDMS gel[4] which provided a $CDCl_3$ line splitting of 20.5 Hz.

^{1}H,^{1}H-NOESY and ^{1}H,^{13}C-HSQC-NOESY spectra (due to severe signal overlap) of a 270 mM sample of **2** were recorded in $CDCl_3$ at 273 K.

NMR data were processed and evaluated with Bruker´s TOPSPIN 2.1 and the included DAISY program was used for spectra simulation whenever necessary. NOESY spectra were integrated and evaluated with AUREMOL;[5] its REFINE module was used for full relaxation matrix calculations.

Assignments of proton and carbon resonances of the conformations with Xxx-Pro *trans*-peptide bonds of **1** and **2** were obtained by the use of one- and two-dimensional NMR spectra. ^{1}H-spectra and ^{13}C-spectra (gated decoupled, power-gated, DEPT-135) in combination with ^{1}H,^{1}H-COSY, ^{1}H,^{1}H-NOESY, ^{1}H,^{13}C-HSQC and ^{1}H,^{13}C-HMBC allowed for almost complete assignment of all resonances of **1** and **2** (Table S1).

MD simulations were performed with CNS 1.1 (Crystallography & NMR System).[6] The simulated annealing protocol included a high temperature stage (2,000 steps at 50,000 K of 7.5 fs each) in torsion angle space, an annealing stage to 0 K (2,000 250 K-steps of 7.5 fs each) and a final energy minimization following the conjugate gradient method in ten cycles of 200 steps each.

The unnatural amino acid *cis*-*b*-ACC was implemented into CNS on the basis of the DFT minimized structures, as discussed in 2.2, and force field parameters were created by the Dundee PRODRG2 Server[7] and XPLO2D.[8] The benzyl protecting group was parameterized on the basis of the available data for the natural amino acid phenylalanine.

The solvent for structure refinement was simulated by a cubic box of 50 Å length filled with 1,000 molecules of chloroform (obtained from VEGA ZZ 2.0.8[9]), for which periodic boundary conditions were assumed. The $CHCl_3$ geometry as well as atomic charges were taken from literature data[10] and force field parameters were generated by XPLO2D.

Calculated structures were visualized and evaluated with MOLMOL 2K.2.[11]

2. Additional Information

2.1 Nomenclature of **1**

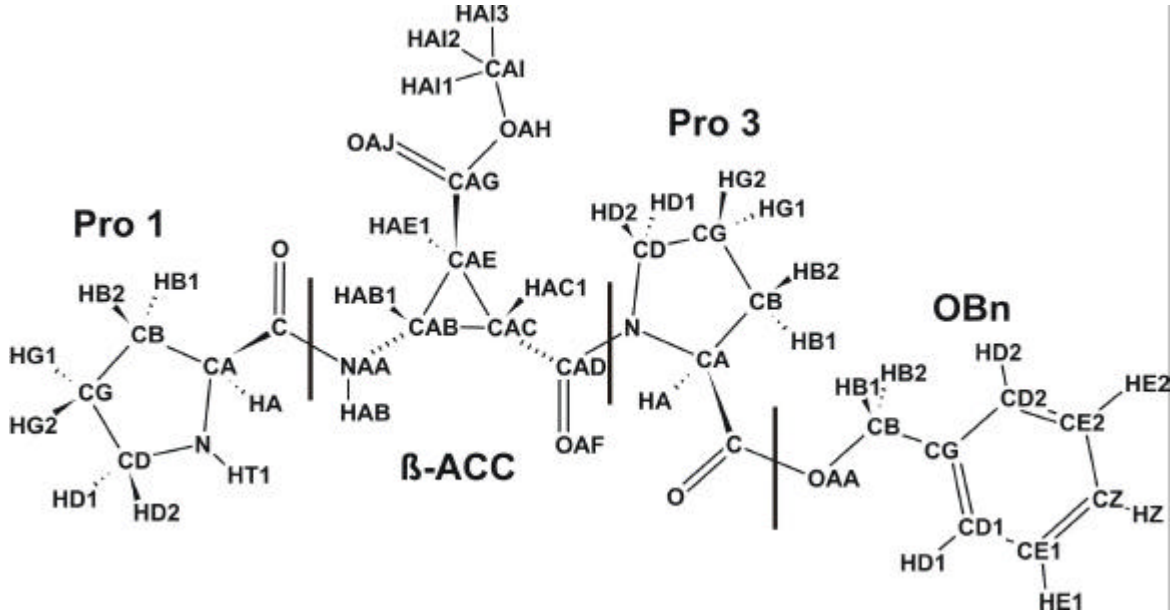

Figure S1. Nomenclature of **1** as used for CNS and within this supporting information. The same atom names were used for **2**. Only the primarily populated conformation of **1** (with a *trans* Xxx-Pro peptide bond) is depicted as only this one was investigated in detail.

2.2 Resonance assignment of **1** and **2**

Table S1. Assignment of proton and carbon resonances of **1** and **2** (major conformation with *trans* peptide bonds only, see Figure S1 for atom nomenclature). Chemical shifts were referenced to solvent signals ($\delta(^1H)_{CHCl3}$ = 7.26 ppm, $\delta(^{13}C)_{CDCl3}$ = 77.16 ppm).

resonance assignment of 1 ($CDCl_3$, 298 K/300 K)				
amino acid	**proton**	**d(^{1}H) / ppm**	**carbon**	**d(^{13}C) / ppm**
Pro 1	HT1	2,08	C	176,4
	HA	3,70	CA	60,8
	HB1	2,07	CB	30,8
	HB2	1,91		
	HG1	1,59	CG	26,2
	HG2	1,69		
	HD1	2,87	CD	47,2
	HD2	2,81		
b-ACC	HAB	8,58	CAD	167,1
	HAB1	4,12	CAB	36,6
	HAC1	2,58	CAC	26,1
	HAE1	2,44	CAE	28,0
			CAG	171,2
	HAI*	3,69	CAI	52,4
Pro 3			C	171,6
	HA	4,55	CA	59,1
	HB1	2,17	CB	29,3
	HB2	2,00		
	HG1	2,01; 2,06	CG	24,7
	HG2			
	HD1	3,65	CD	47,5
	HD2	3,87		
OBn	HB1	5,09; 5,12	CB	66,7
	HB2			
			CG	135,7
	HD*	7,32	CD*	128,1
	HE*	7,34	CE*	128,7
	HZ	7,31	CZ	128,4

resonance assignment of 1 ($CDCl_3$, 240 K)				
amino acid	**proton**	**d(^{1}H) / ppm**	**carbon**	**d(^{13}C) / ppm**
Pro 1	HT1	---	C	176,2
	HA	3,75	CA	59,9
	HB1	2,09	CB	30,4
	HB2	1,90		
	HG1	1,59	CG	26,0
	HG2	1,68		
	HD1	2,87	CD	46,8
	HD2	2,74		
b-ACC	HAB	8,97	CAD	166,8
	HAB1	4,18	CAB	36,2
	HAC1	2,61	CAC	25,4
	HAE1	2,46	CAE	27,8
			CAG	171,0
	HAI*	3,67	CAI	52,4
Pro 3			C	171,2
	HA	4,53	CA	58,5
	HB1	2,17	CB	28,8
	HB2	2,00		
	HG1	2,02-2,05	CG	24,3
	HG2			
	HD1	3,65	CD	47,2
	HD2	3,91		
OBn	HB1	5,04; 5,09	CB	66,5
	HB2			
			CG	134,8
	HD*	7,34	CD*	127,9
	HE*	7,36	CE*	128,4
	HZ	7,33	CZ	128,2

resonance assignment of 2 ($CDCl_3$, 273 K)				
amino acid	**proton**	**d(^{1}H) / ppm**	**carbon**	**d(^{13}C) / ppm**
Pro 1	HT1	---	C	---
	HA	3,89	CA	58,8
	HB1	2,15	CB	30,1
	HB2	1,80		
	HG1	1,81	CG	26,0
	HG2	1,73		
	HD1	2,92	CD	47,3
	HD2	3,13		
Pro 2			C	---
	HA	4,53	CA	59,9
	HB1	1,90	CB	27,5
	HB2	2,19		
	HG1	1,88-1,92	CG	24,7
	HG2			
	HD1	3,47	CD	46,5
	HD2	3,40		
b-ACC	HAB	7,65	CAD	---
	HAB1	3,91	CAB	35,8
	HAC1	2,52	CAC	26,5
	HAE1	2,31	CAE	28,2
			CAG	---
	HAI*	3,65	CAI	52,2
OBn	HB1	5,06; 5,08	CB	66,9
	HB2			
			CG	134,8
	HD*	7,31	CD*	127,9
	HE*	7,33	CE*	128,4
	HZ	7,31-7,32	CZ	128,3

2.3 Quality check of different *cis-b*-ACC coordinates with RDC data

In order to generate an appropriate β-ACC parametrization for MD simulations, various *cis-b*-ACC coordinate files were generated with the help of the Spartan 06 program package[12] (Table S2). Three different starting structures were used for that purpose: one structure that was directly built within Spartan, a second structure which was generated by the Dundee PRODRG2 Server, and a third one by inverting the stereocenters of a crystal structure of the enantiomer of **3**[13] followed by addition of hydrogen atoms with Spartan. Different equilibrium geometry calculation algorithms were applied to these structures: a molecular mechanics approach (MMFF force field), a semi-empirical calculation (RM1 method) and an *ab initio* calculation (Hartree-Fock with 6-31G* basis set). In addition, density functional theory calculations (B3LYP, 6-31G* basis set) on the crystal structure and its MM minimized offspring were performed. All these structures were fitted to 6 RDCs within the rigid β-ACC moiety with the help of the PALES[14, 15] bestFit module (using singular-value decomposition). The results in terms of alignment tensors and bond and angle parameters as well as quality factors Q are summarized in Figure S2 and Table S2 (see footnote of Table S2 for structure code).

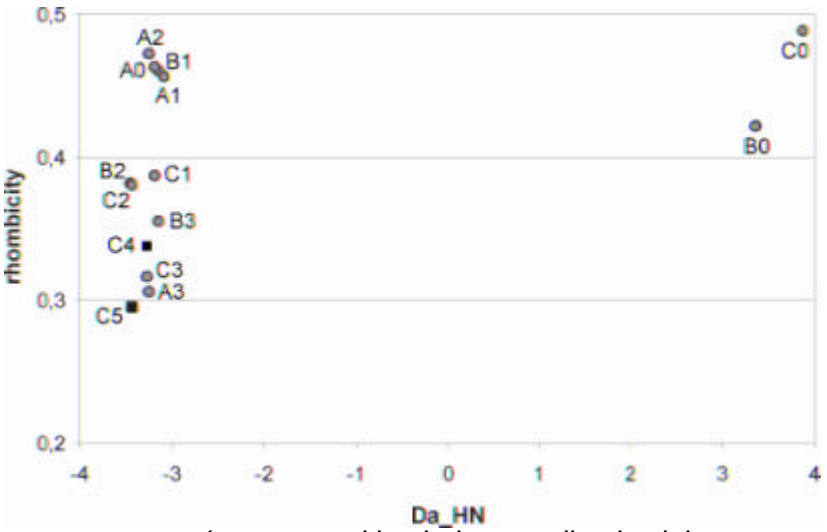

Figure S2. Alignment tensors (represented by their normalized axial components and their rhombicities)based on experimental β-ACC RDCs and the 14 different coordinate sets of 3 (see Table S2).

It can be concluded that B0 and C0 (the PRODRG structure and the crystal structure to which hydrogen atoms had been added simply by Spartan) yielded insufficient Q factors and erroneous alignment tensors due to the wrong hydrogen positions (decisive parameters are highlighted in Table S2). All the other equilibrium geometry calculation methods, however, resulted in acceptable Q factors and both similar parameters and alignment tensors within the range of experimental errors. The two geometries obtained by the DFT calculations were used as the basis for the applied CNS parametrization of *cis-b*-ACC.

Table S2. Comparison of geometric parameters of the generated β-ACC coordinates of **1** and their RDC evaluation with PALES.

bond lengths / Å

		A0	A1	A2	A3	B0	B1	B2	B3	C0	C1	C2	C3	C4	C5
CA	CAC	1,56	1,51	1,53	1,50	1,56	1,51	1,53	1,50	1,47	1,51	1,53	1,50	1,52	1,52
CA	CAE	1,56	1,52	1,52	1,51	1,57	1,52	1,53	1,52	1,54	1,52	1,53	1,51	1,52	1,52
CA	CAE	1,56	1,51	1,53	1,50	1,56	1,51	1,53	1,50	1,51	1,51	1,53	1,49	1,54	1,50
CA	NAA	1,47	1,44	1,44	1,42	1,51	1,43	1,43	1,42	1,44	1,44	1,43	1,42	1,42	1,43
CA	CAD	1,53	1,48	1,50	1,50	1,58	1,49	1,49	1,50	1,48	1,49	1,50	1,50	1,50	1,51
CA	CAG	1,53	1,49	1,49	1,50	1,56	1,48	1,48	1,49	1,50	1,48	1,48	1,49	1,49	1,49
CA	HAB	1,10	1,09	1,11	1,07	1,00	1,09	1,11	1,07	1,10	1,09	1,11	1,07	1,08	1,08
CA	HAC	1,10	1,09	1,11	1,07	1,00	1,09	1,11	1,07	1,10	1,09	1,10	1,07	1,08	1,08
CA	HAE	1,10	1,09	1,11	1,07	1,00	1,09	1,11	1,07	1,10	1,09	1,11	1,07	1,09	1,09
NA	HAB	1,01	1,01	1,01	1,00	1,00	1,02	1,02	1,00	1,01	1,02	1,02	1,00	1,02	1,01

bond angles / °

			A0	A1	A2	A3	B0	B1	B2	B3	C0	C1	C2	C3	C4	C5
CAB	CA	CAE	60,0	59,8	60,1	60,0	59,8	59,5	60,0	59,7	60,3	59,7	60,0	59,3	59,5	59,2
CAC	CA	CAB	60,0	59,8	60,2	59,5	60,0	60,1	60,2	59,3	57,5	60,0	60,2	60,1	59,5	60,2
CAE	CA	CAC	60,0	60,4	59,7	60,6	60,2	60,4	59,8	61,0	62,2	60,3	59,9	60,6	61,0	60,6
NAA	CA	CAC	117,	121,	118,	121,	121,	121,	119,	112,	118,	121,	118,	121,	121,	120,
NAA	CA	CAE	117,	121,	118,	121,	121,	121,	117,	121,	116,	121,	117,	118,	120,	119,
CAD	CA	CAB	117,	121,	119,	121,	122,	122,	118,	120,	118,	120,	117,	118,	118,	117,
CAD	CA	CAE	117,	118,	117,	117,	121,	118,	117,	116,	119,	119,	117,	116,	115,	115,
CAG	CA	CAB	117,	120,	116,	118,	122,	119,	116,	118,	123,	119,	118,	120,	120,	120,
CAG	CA	CAC	117,	117,	116,	117,	121,	119,	116,	117,	119,	120,	119,	120,	120,	121,
HAB	CA	CAC	117,	116,	118,	114,	135,	116,	116,	115,	135,	116,	117,	115,	116,	115,
HAB	CA	CAE	117,	116,	119,	115,	134,	117,	118,	115,	133,	116,	119,	117,	117,	117,
HAC	CA	CAB	117,	116,	118,	113,	134,	114,	117,	113,	135,	116,	119,	115,	115,	115,
HAC	CA	CAE	117,	115,	118,	113,	135,	118,	117,	114,	134,	115,	117,	116,	114,	116,
HAE	CA	CAB	117,	113,	118,	114,	134,	115,	119,	116,	134,	117,	120,	117,	116,	117,
HAE	CA	CAC	117,	118,	119,	115,	135,	117,	120,	116,	137,	117,	119,	115,	115,	114,
HAB	CA	NAA	116,	111,	113,	113,	88,4	112,	113,	112,	93,0	112,	113,	113,	111,	113,
HAC	CA	CAD	116,	113,	113,	118,	87,3	114,	115,	118,	91,7	114,	114,	118,	119,	118,
HAE	CA	CAG	116,	115,	115,	118,	87,7	114,	114,	116,	88,1	112,	110,	112,	113,	113,

PALES-output

	A0	A1	A2	A3	B0	B1	B2	B3	C0	C1	C2	C3	C4	C5
Q RDC_RMS	0,05	0,09	0,08	0,03	0,35	0,03	0,06	0,05	0,31	0,06	0,05	0,00	0,02	0,03
Da_HN	-3,18	-3,07	-3,25	-3,23	3,37	-3,13	-3,44	-3,14	3,87	-3,19	-3,42	-3,27	-3,27	-3,43
rhombicity	0,46	0,46	0,47	0,30	0,42	0,46	0,38	0,35	0,49	0,39	0,38	0,32	0,34	0,29

Structure code:

A	structure built within Spartan
B	PRODRG structure
C	crystal structure
C4	DFT: B3LYP, 6-31G*, starting from C0
C5	DFT: B3LYP, 6-31G*, starting from C1

0	starting structure
1	molecular mechanics: MMFF
2	semi-empirical: RM1
3	Hartree-Fock: 6-31G*

2.4. Structure investigation of **1**

2.4.1 Structure investigation of **1** at 240 K

28 negative NOE contacts (spin diffusion limit), detected in 2D ^{1}H,^{1}H-NOESY (350 ms mixing time) spectra at 240 K, were used as restraints in MD simulations. At first, relatively loose distance restraints were used to restrict the available conformational space, employing uniform upper and lower bounds of 0.500 nm and 0.175 nm, respectively. Using the standard simulated annealing protocol, described in chapter 1.3, 100 structures were calculated. Of these, 5 structures with low total

and NOE energies were selected as a representative set for further analysis. Each member of this ensemble together with the NOESY crosspeak volumes (determined with AUREMOL) was used as input for the full relaxation matrix calculation (with the REFINE module (to be published) included in AUREMOL) in order to take spin diffusion effects into account. The refined sets of distance restraints were then applied for the next round of structure calculations. In total 5 rounds of structure calculations were performed until convergence of both distance restraints and calculated structures was reached. Solvent refined structures were obtained by subsequent refinement employing a chloroform box with periodic boundary conditions. Figure S3 shows the obtained structure ensemble.

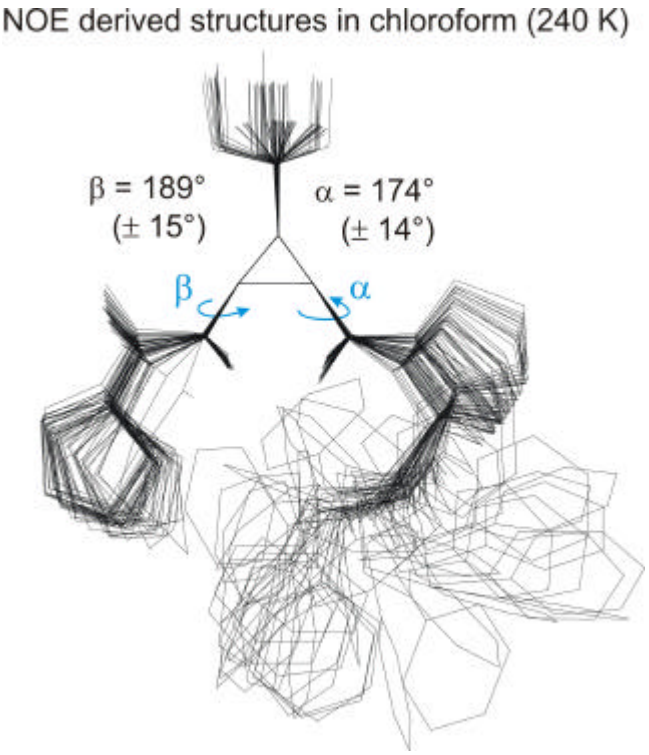

Figure S3. Ensemble of 50 structures refined in a chloroform box with 28 NOE distance restraints at 240 K derived from full relaxation matrix calculations.

The range of the β angle populated by the structure ensemble is in agreement with the large *J*-coupling between the amide proton and the β-proton of *cis*-*b*-ACC (9.69 Hz at 240 K). As no Karplus curve has become available for *cis*-*b*-ACC so far, the quantum-mechanically calculated Karplus curve for **4**[16] was compared to the one calculated for **5** by an empirically generalized Karplus equation.[17]

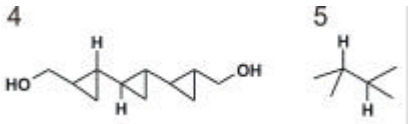

Thus, it was concluded that the cyclopropane ring scales down the scalar coupling constant in comparison to aliphatic chains as substituents. This was transferred onto the well-known Karplus curve for $^{3}J(H^{N}H^{\alpha})$ of natural α-amino acids.[18] Hence, the observed *J* coupling of 9.69 Hz was interpreted in terms of a population of β values of 180° ± 30° (Figure 2B).

2.4.2 Structure investigation of **1** at 300 K based on NOEs

At 300 K, only four NOEs carrying quantifiable α- and β-relevant structural information could be identified (HAC1 - HD*(Pro3) for α and HAB - HAC1 as well as HAB - HAE1 for β). The quantification of this NOE information was additionally hampered by chemical exchange processes involving the amide proton. Therefore, no global calibration of NOE intensities was possible at 300 K and the REFINE module of AUREMOL could not be applied for spin diffusion corrections either.

When trying to translate relative NOE intensities relevant for α directly into angular information as shown in Figure 2B (right), proline side chain conformations become important as they influence interatomar distances, too. In order to take this into account, a two-state approximation was made for Pro 3 (the two conformations of low energy are usually referred to as “up” and “down”)[19] and the population of these two conformations was estimated to be approximately 30 % : 70% up : down with the help of *J* couplings.[20] This ratio was used for the theoretical calculation of NOE intensities (Figure 2B, it was also used for Figure 2D) which includes the assumption that the populations of α and proline side chain conformations are independent.

In order to additionally obtain upper limit distance restraints for MD simulations, the structurally relevant four NOEs that carry conformational information about the angles α and β were quantified according to equation 1: Two β-relevant contacts involving the amide proton were calibrated to the NOE HAB-HAB1 (r_{ref} = 3.0 Å) whose distance cannot exceed 3 Å so that the applied restraints represent upper limits on any account. Two further restraints, meaningful for α, were calibrated to the geminal peak of the δ-protons of Pro 3. The upper limit of all these restraints was extended to $1.07*r_{ref}$ (~ $1.5*NOE_{ref}/NOE_{XY}$) in order to concede spin diffusion influences and shortcomings in NOE integration. The generated structure ensemble is displayed in Figure 3A in the communication.

$$r_{XY} = r_{ref} \cdot \left(\frac{NOE_{ref}}{NOE_{XY}} \right)^{\frac{1}{6}} \qquad (1)$$

2.4.3 Structure investigation of **1** at 298 K based on RDCs

A second set of structures was calculated employing residual dipolar couplings (RDCs) as conformational restraints. 23 RDCs could be determined experimentally from well-resolved 1D proton spectra and P.E.HSQC spectra at 298 K. They are summarized together with their estimated errors in Table S3. However, only 8 of them (highlighted in Table S3) were suited for interpretation as all the others were heavily influenced by internal dynamics.
Experimental errors of 0.2 Hz were assumed for $^3D_{HH}$ determined from multiplet analysis of 1D proton spectra. For $^1D_{CH}$ from P.E.HSQC spectra, the error was estimated to be 1 Hz in case the RDC could be extracted directly from peak splitting in ω2 and 2 Hz in case the multiplets in ω2 had to be simulated with DAISY due to higher order influences. Errors in $^2D_{HH}$ from the peak tilt in P.E.HSQC spectra were estimated dependent on the peak quality as 0.4 Hz or 0.7 Hz. These errors were also used for the alignment tensor determination and Q calculation with PALES.

Table S3. Experimentally determined residual dipolar couplings.

				D / Hz	ΔD / Hz	source
Pro 1	$^1D_{CH}$	CA	HA	**0,1**	**1,0**	P.E.HSQC
		CB	HB1	**0,5**	**1,0**	P.E.HSQC
			HB2	**2,7**	**1,0**	P.E.HSQC
		CG	HG1	**2,6**	**1,0**	P.E.HSQC
			HG2	**3,7**	**1,0**	P.E.HSQC
		CD	HD1	**-0,8**	**1,0**	P.E.HSQC
			HD2	**-1,1**	**1,0**	P.E.HSQC
	$^2D_{HH}$	HB1	HB2	**2,9**	**0,4**	P.E.HSQC
		HG1	HG2	**3,8**	**0,4**	P.E.HSQC
		HD1	HD2	**2,0**	**0,4**	P.E.HSQC
b-ACC	$^1D_{CH}$	CAB	HAB1	**-7,4**	**1,0**	P.E.HSQC
		CAC	HAC1	**5,2**	**2,0**	P.E.HSQC
		CAE	HAE1	**2,9**	**2,0**	P.E.HSQC
	$^3D_{HH}$	HAB	HAB1	**-0,9**	**0,2**	1D-^{1}H
		HAB1	HAC1	**-0,3**	**0,2**	1D-^{1}H
		HAB1	HAE1	**0,5**	**0,2**	1D-^{1}H
		HAC1	HAE1	**1,8**	**0,2**	1D-^{1}H
Pro 3	$^1D_{CH}$	CA	HA	**5,0**	**1,0**	P.E.HSQC
		CD	HD1	**-1,9**	**1,0**	P.E.HSQC
			HD2	**-0,3**	**1,0**	P.E.HSQC
	$^2D_{HH}$	HD1	HD2	**3,7**	**0,7**	P.E.HSQC
	$^3D_{HH}$	HA	HB1	**3,0**	**0,2**	1D-^{1}H
			HB2	**1,3**	**0,2**	1D-^{1}H

Concerning the angle α, the RDCs $^2D(H^{\delta2}H^{\delta3})$, $^1D(C^{\delta}H^{\delta2})$, $^1D(C^{\delta}H^{\delta3})$ and $^1D(C^{\alpha}H^{\alpha})$ bear conformational information, but in principle they all depend on the proline side chain conformation which impedes their straightforward interpretation. However, $^1D(C^{\alpha}H^{\alpha})$ shows almost no dependence on the proline side chain conformation (Figure S4) and is therefore suited to extract information on α.

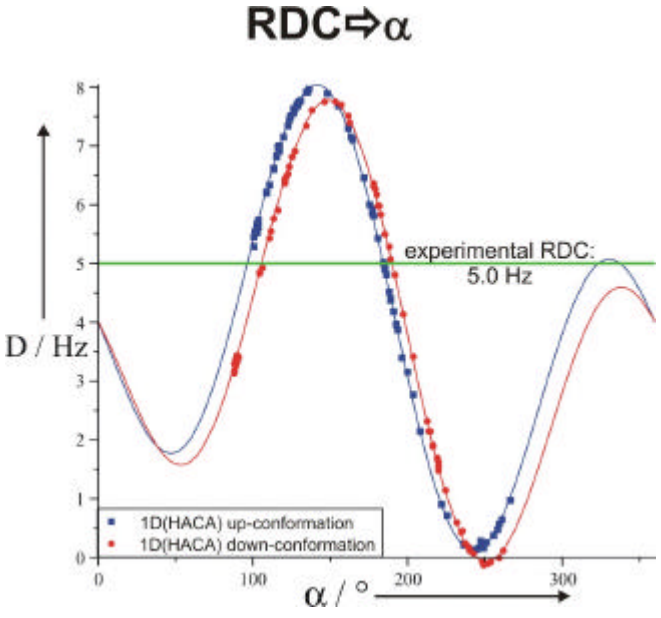

Figure S4. $^1D(C^{\alpha}H^{\alpha})$ shows almost no dependence on the side chain conformation of Pro 3. (A ratio of 30:70 up:down was used for Figure 2D.)

For the use of RDCs as CNS restraints, the alignment tensor defined for the *cis*-*b*-ACC residue was applied. As the "axial" input in CNS is dependent on D_{max}, i.e. on the internuclear distance, three different scaling factors for the "axial" value of $^{3}D(H^{N}H^{\beta})$ (the only applied RDC for which the distance cannot be assumed to be fixed) were used which were supposed to cover the available distance range. However, the structures of low energy generated with these three different scaling factors were identical, resulting in the 40 structures (out of 300) that are displayed in the communication.

2.5 Structure investigation of **2** at 273 K

54 positive NOE contacts (extreme narrowing limit) detected in $^{1}H,^{1}H$-NOESY (350 ms mixing time) spectra at 273 K were used as restraints in MD simulations employing a procedure analogue to **1** (chapter 2.3). Because of similar chemical shifts of some protons and therefore ambiguous assignment of some NOESY peaks a $^{1}H,^{13}C$-HSQC-NOESY was measured. Nevertheless, eight NOESY contacts remained ambiguous and one twofold ambiguous. All NOESY contacts to the aromatic protons have been included only qualitatively with uniform upper and lower bounds of 0.500 nm and 0.175 nm, respectively. Of the 54 NOE contacts, four had to be replaced by corresponding signals from other NOESY spectra because of poor peak quality. These peaks were checked carefully and their upper and lower bounds were extended by 0.02 nm.

The relatively high number of restraints for such a small peptide and especially the high number of long range contacts (Figure S5) leads to very well defined final structures (Scheme 2 in the communication).

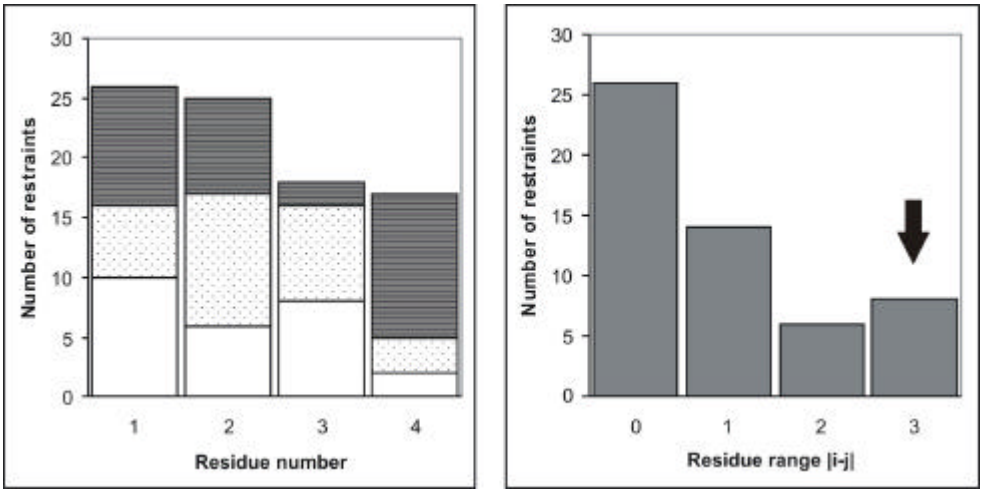

Figure S5. Distance restraints of **2**. Left: For each residue white = intraresidual; pale grey = i+|i+1|; dark grey = long range restraints. Right: Restraints for the whole molecule vs. the distance between the interacting residues.

The calculated structures of **2** have already converged after two cycles of structure calculations (Figure S6). This can be interpreted, in addition to the high number of restraints, in terms of a very good reliability of the calculated structures.

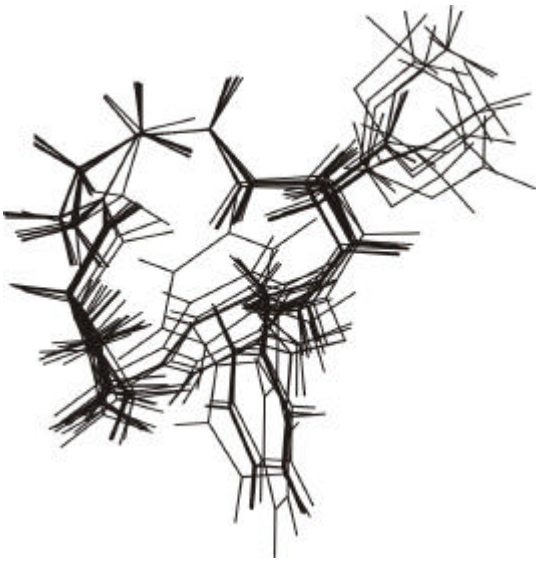

Figure S6. Ensemble of the lowest energy structures of **2** for each step in the spin diffusion cycle. The structures are self-consistent.

Small changes in the chemical shifts (< 0.72 ppm) show that this conformation is still preferred at higher temperatures.

Table S4: temperature dependent changes in ^{13}C chemical shifts.

		300 K - 273 K	300 K - 270 K	300 K - 240 K	273 K - 270 K	273 K - 240 K	270 K - 240 K
Pro 1	C	---	0,44	---	---	---	---
	CA	0,56	0,33	0,58	0,23	0,02	0,25
	CB	0,41	0,05	0,08	0,36	-0,33	0,03
	CG	0,72	0,38	0,35	0,34	-0,37	-0,03
	CD	0,36	0,05	0,03	0,31	-0,33	-0,02
Pro 2	C	---	-0,01	0,07	---	---	0,08
	CA	0,31	0,01	0,13	0,3	-0,18	0,12
	CB	0,19	-0,01	-0,03	0,2	-0,22	-0,02
	CG	0,24	0	0,09	0,24	-0,15	0,09
	CD	0,18	-0,05	0,02	0,23	-0,16	0,07
β-ACC	C	---	-0,17	-0,26	---	---	-0,09
	CA	-0,04	-0,1	0,14	0,06	0,18	0,24
	CB	0,26	-0,02	0,02	0,28	-0,24	0,04
	CG	0,33	-0,04	0	0,37	-0,33	0,04
	CD	---	-0,15	-0,22	---	---	-0,07
	CE	0,08	-0,24	-0,39	0,32	-0,47	-0,15
OBn	CB	0,26	-0,1	-0,12	0,36	-0,38	-0,02
	CG	0,5	0,24	0,57	0,26	0,07	0,33
	CD	0,27	-0,11	-0,21	0,38	-0,48	-0,1
	CE	0,24	-0,06	-0,04	0,3	-0,28	0,02
	CZ	0,2	-0,12	-0,17	0,32	-0,37	-0,05

Analogously to **1**, the range of the β angle populated by the structure ensemble of **2** (221° ± 17°) is in very good agreement with the *J*-coupling between the amide proton and the β-proton of *cis*-*b*-ACC (6.63 Hz at 273 K) which indicates β values between 225° ±15° (following to the estimation procedure described in chapter 2.3).

All distances shorter than 3,5 Å that occurred in more than the half low-energy CNS structures give rise to crosspeaks in the NOESY spectra.

Table S5. All H-H distances < 3.5 Å in the calculated structures of **2** are represented by an NOESY crosspeak.

H-H-distances in calculated structures < 3,5 Å						NOESY crosspeaks	used as distance restraints
1	PRO	HA	2	PRO	HD1	yes	yes
1	PRO	HA	2	PRO	HD2	yes	yes
1	PRO	HB1	2	PRO	HD1	yes	yes
1	PRO	HB1	2	PRO	HD2	yes	yes
1	PRO	HB1	4	BZA	HD2	yes	yes
1	PRO	HB2	2	PRO	HD1	yes	yes
1	PRO	HB2	2	PRO	HD2	yes	yes
1	PRO	HB2	3	β-ACC	HAB	yes	yes
1	PRO	HB2	4	BZA	HB1	yes	yes
1	PRO	HB2	4	BZA	HB2	yes	yes
1	PRO	HB2	4	BZA	HD2	yes	yes
1	PRO	HB2	4	BZA	HD1	yes	yes
1	PRO	HB2	4	BZA	HE2	yes	yes
1	PRO	HG2	3	β-ACC	HAB	yes	yes
1	PRO	HG2	4	BZA	HB1	yes	yes
1	PRO	HG2	4	BZA	HB2	yes	yes
1	PRO	HG2	4	BZA	HD2	yes	yes
2	PRO	HB2	3	β-ACC	HAB	yes	yes
2	PRO	HB2	4	BZA	HB1	t1 noise	---
2	PRO	HB2	4	BZA	HD1	very small	---
2	PRO	HB1	4	BZA	HE1	yes	yes
2	PRO	HG2	4	BZA	HD1	yes	yes
2	PRO	HG2	4	BZA	HE1	yes	yes
2	PRO	HG2	4	BZA	HZ	yes	yes
2	PRO	HD2	3	β-ACC	HAB	yes	yes
2	PRO	HD2	4	BZA	HB1	yes	yes
2	PRO	HD2	4	BZA	HD1	yes	yes
2	PRO	HD2	4	BZA	HE1	overlap	---
2	PRO	HD2	4	BZA	HZ	yes	yes
3	β-ACC	HAB	4	BZA	HB1	small	---
3	β-ACC	HAB	4	BZA	HB2	small	---
3	β-ACC	HAB	4	BZA	HD1	near diag.	---
3	β-ACC	HAB1	4	BZA	HB2	t1 noise	---
3	β-ACC	HAC1	4	BZA	HB2	yes	yes
3	β-ACC	HAC1	4	BZA	HB1	yes	c

2.6 Statistical information on the calculated structures of **1** and **2**

Table S6. Statistical information on the calculated structure ensembles displayed in the communication and the supporting information**.**

	Scheme 2B	Figure S3	Figure 3A	Figure 3B
number of selected structures	50	50	40	40
number of restraints (NOE/RDC, respectively)	54	28	4	11
rmsd (heavy atoms without BZA residue) / Å	0,39 ± 0,27	0,61 ± 0,24	0,52 ± 0,20 *	0,31 ± 0,14 *
E(NOE/RDC) / kJ/mol	2,0 ± 0,1	1,4 ± 1,8	< 1	< 1
E(total) / kJ/mol	39,2 ± 0,1	-153,0 ± 11,3	12,0 ± 0,2	19,7 ± 2,6

*only those heavy atoms being directly affected by the applied restraints were concerned for rmsd calculation.

[1] V. D'Elia, H. Zwicknagl, O. Reiser, *J. Org. Chem.* **2008**, *73*, 3262.
[2] A. Jerschow, N. Müller, *J. Magn. Reson.* **1997**, *125*, 372.
[3] P. Tzvetkova, S. Simova, B. Luy, *J. Magn. Reson.* **2007**, *186*, 193.
[4] J. C. Freudenberger, P. Spiteller, R. Bauer, H. Kessler, B. Luy, *J. Am. Chem. Soc.* **2004**, *126*, 14690.
[5] W. Gronwald, H. R. Kalbitzer, *Prog. Nucl. Magn. Reson. Spectrosc.* **2004**, *44*, 33.
[6] A. T. Brünger, P. D. Adams, G. M. Clore, W. L. DeLano, P. Gros, R. W. Grosse-Kunstleve, J.-S. Jiang, J. Kuszewski, M. Nilges, N. S. Pannu, R. J. Read, L. M. Rice, T. Simonson, G. L. Warren, *Acta Cryst.* **1998**, *D54*, 905.
[7] A. W. Schüttelkopf, D. M. F. van Aalten, *Acta Cryst.* **2004**, *D60*, 1355.
[8] G. J. Kleywegt, K. Henrick, E. J. Dodson, D. M. F. van Aalten, *Structure* **2003**, *11*, 1051.
[9] A. Pedretti, L. Villa, G. Vistoli, *J. Comput.-Aided Mol. Des.* **2004**, *18*, 167.
[10] M. E. Martín, A. Muñoz Losa, I. F. Galván, M. A. Aguilar, *J. Mol. Struct. (THEOCHEM)* **2006**, *775*, 81.
[11] R. Koradi, M. Billeter, K. Wüthrich, *J. Mol. Graphics* **1996**, *14*, 51.
[12] http://www.wavefun.com.
[13] C. Zorn, Ph.D. thesis, Universität Regensburg (Regensburg), **2001**.
[14] M. Zweckstetter, *Nat. Protoc.* **2008**, *3*, 679.
[15] M. Zweckstetter, A. Bax, *J. Am. Chem. Soc.* **2000**, *122*, 3791.
[16] A. G. M. Barrett, R. A. James, G. E. Morton, P. A. Procopiou, C. Boehme, A. deMeijere, C. Griesinger, U. M. Reinscheid, *J. Org. Chem.* **2006**, *71*, 2756.
[17] C. A. G. Haasnoot, F. A. A. M. de Leeuw, C. Altona, *Tetrahedron* **1980**, *36*, 2783.
[18] V. F. Bystrov, *Prog. Nucl. Magn. Reson. Spectrosc.* **1976**, *10*, 41.
[19] G. N. Ramachandran, A. V. Lakshminarayanan, R. Balasubramanian, G. Tegoni, *Biochim. Biophys. Acta, Prot. Struct.* **1970**, *221*, 165.
[20] M. Schmid, diploma thesis, Universität Regensburg (Germany), **2007**.